ChemComm

Accepted Manuscript

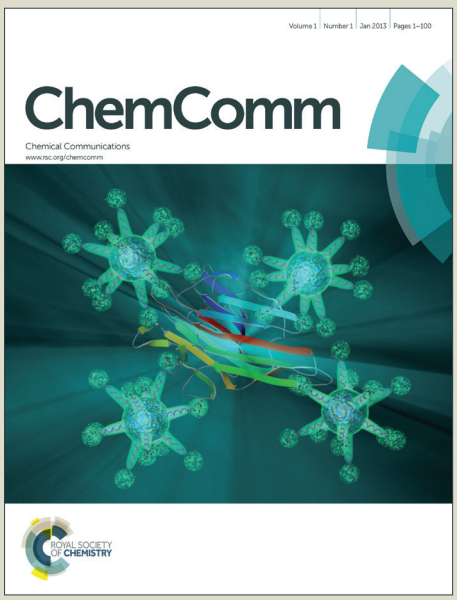

ROYAL SOCIETY OF CHEMISTRY

www.rsc.org/chemcomm

ChemComm

RSCPublishing

COMMUNICATION

An injectable thermogel with high radiopacity

Cite this: DOI: 10.1039/x0xx00000x

Kewen Lei, Wenjia Shen, Luping Cao, Lin Yu*, Jiandong Ding

Received 00th January 2015,
Accepted 00th January 2015

DOI: 10.1039/x0xx00000x

www.rsc.org/

An injectable PEG/polyester thermogel with strong X-ray opacity was designed and synthesized through the conjugation of 2, 3, 5-triiodobenzoic acid to the hydrophobic end of mPEG-PLA diblock copolymer for the first time.

Thermogelling polymers based on poly(ethylene glycol) (PEG) and biodegradable polyesters, such as poly(lactic acid-co-glycolic acid) (PLGA), poly(lactic acid) (PLA), poly(caprolactone) (PCL), poly(caprolactone-co-lactic acid) (PCLA) and poly(caprolactone-co-glycolic acid) (PCGA), have been suggested as very promising biomaterials for sustained drug delivery, injectable tissue engineering, prevention of post-surgical adhesion, and so on.[1] Typically, these polymers are able to dissolve in water at low temperature, such as 20 °C, and exhibit reversible sol-gel transition with increase of temperature. Drugs or cells are easily incorporated into the polymer aqueous solutions by simply mixing them without using any organic solvents. The corresponding formulations can be injected into the body using a conventional syringe and then an *in situ* physical hydrogel is spontaneously formed at body temperature, acting as a sustained drug delivery depot or a cell-growing matrix.[2] The thermogelation of such a system is attributed to the delicate balance between hydrophilicity of PEG block and hydrophobicity of polyester segment.[3] Their thermogelling properties and degradation behaviors can be well-adjusted by composition of polyester, PEG/polyester ratio, block length, molecular weight distribution and polymer concentration.[4] In particular, end-group modification from hydroxyl groups to alkyl groups even can determine the macroscopic physical gelation of polyester-PEG-polyester triblock copolymers in water.[4b, 5]

As an implanted biomaterial, *in-situ* detection of thermogel formation at body sites, such as joints and vessels, and corresponding acquirement of more insights into *in vivo* behaviors of thermogels are very meaningful for fundamental research of biomaterials and their clinical applications. Fluorescent imaging is one of commonly used methods for non-invasive detection *in vivo*,[6] whereas the penetration depth of light used in fluorescent imaging limited its *in vivo* application to a large extent.[7] Computed tomography (CT) affords an alternative technique but is relatively less developed. Compared with fluorescent imaging, X-ray CT has the capacity to penetrate through the entire body and reconstruct three dimensional (3D) volume of implanted devices/materials deep within the body,[7, 8] and thus is very convenient for *in vivo* visualized detection and morphology analysis of the implants.

To date, only a few of radiopaque hydrogel systems have been developed. For example, Lerouge et al directly incorporated commercial iodine contrast agents into chitosan-based hydrogels. It is, however, impossible to longitudinally trace the hydrogel *in vivo* due to the rapid leaking of contrast agents from hydrogel matrix within several hours.[9] To circumvent this problem, iodine-containing moieties have been tried to covalently link with polymers. For instance, mixing of a 2, 3, 5-triiodobenzoic acid (TIB)-capped PCLA-PEG-PCLA triblock copolymer with another similar polymer capped with acetyl moieties led to the formation of an *in situ* radiopaque hydrogel at temperatures below 10-15 °C; yet the integrity of such a hydrogel was not maintained at body temperature due to the rapid occurrence of phase-separation.[10]

To the best of our knowledge, no thermogel systems with a strong and long-acting radiopacity has been reported so far. In fact, it is technically challenging to obtain radiopaque PEG/polyester thermogels using covalent linkage of iodine moieties to polymers, because such a system suffers from a dilemma to possess the strong radiopacity and to maintain the sol-gel transition in water. To solve this problem, many efforts have been tried, and such a dilemma was finally overcome by us in the present study, as schematically displayed in Fig. 1. The TIB-capped diblock copolymer of methoxy poly(ethylene glycol) (mPEG) and PLA, mPEG-PLA, with an appropriate mPEG/PLA ratio was found to satisfy both of the above-mentioned requirements, and thus an injectable PEG/polyester thermogel with strong X-ray opacity was obtained. This work is aimed to illustrate our strategy of molecular design, examine the thermogelling behaviors of synthesized polymers, and assess their *in vitro* and *in vivo* radiopacity.

State Key Laboratory of Molecular Engineering of Polymers, Department of Macromolecular Science, Fudan University, Shanghai 200433, China
* Corresponding authors, Tel: +86-21-65642531; fax: +86-21-65640293
E-mail address: yu_lin@fudan.edu.cn (L. Yu)

† Electronic supplementary information (ESI) available: Experimental details and additional figures.

Table 1. mPEG-PLA diblock copolymers, PLA-PEG-PEG triblock copolymer and their TIB-capped derivatives investigated in this study

Sample ID	M_n[a]	M_n[b]	M_w/M_n[b]	TIB substituted percentage[a]	Solubility in water	Sol-gel transition temperature[c]
P1	550-910	1497	1.33	\	soluble	No
P1-TIB	550-1220-500	1650	1.29	100	soluble	No
P2	550-1170	1770	1.43	\	soluble	No
P2-TIB	550-1350-500	1773	1.27	93	soluble	32 °C
P3	550-1600	2043	1.32	\	soluble	14 °C
P3-TIB	550-1780-500	2153	1.24	96	insoluble	\
P4	750-1910	2639	1.49	\	soluble	35 °C
P5	730-1000-730	2906	1.17	\	soluble	No
P5-DiTIB	500-780-1000-780-500	3034	1.14	91	insoluble	\

[a] Number-average molecular weight (M_n) of mPEG or PEG block was provided by Aldrich, M_n of PLA blocks and TIB substituted percentage were calculated via ^{1}H NMR; [b] Measured by GPC, relative to polystyrene standards; [c] Determined via the vial inverting approach. Polymer weight concentration was 40% in water. "No" represents that the polymer aqueous solution at any concentration exhibited just a sol state at a broad temperature range (0-50 °C)

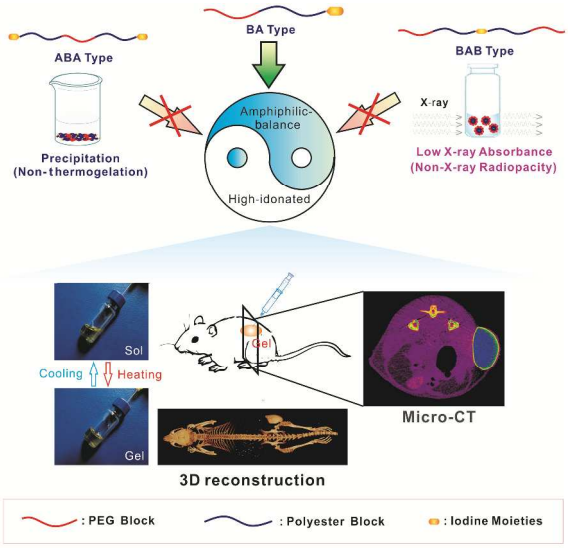

Fig. 1 Schematic presentation of the strategy to design and synthesize radiopaque thermogel. Due to the subtle end-group effect,[4b, 5a] the introduction of iodine-containing moieties to both ends of polyester-PEG-polyester triblock copolymer resulted in its water-insolubility even if the triblock copolymer itself was very hydrophilic. The iodine-containing moieties, such as difunctional 2,3-diiodo-2-butene-1,4-diol, were also assumed as a coupling agent to link with the hydrophobic ends of two mPEG-polyester diblock copolymer molecules. However, the iodine content in the BAB-type polymers obtained might be too low to be visualized by X-ray photography. Fortunately, we revealed that iodine contrast-capped mPEG-polyester diblock copolymer with appropriate mPEG/polyester ratio was soluble in water at room temperature and formed a non-flowing thermogel at body temperature. Both the *in vitro* and *in vivo* examination of such a thermogel using Micro-CT exhibited strong radiopacity.

A series of mPEG-PLA diblock copolymers were synthesized by ring-opening polymerization of D, L-lactide (LA) in the presence of mPEG using stannous octonate as the catalyst, and then TIB was introduced into the PLA end of mPEG-PLA diblock copolymer by esterification between the end-hydroxyl group of mPEG-PLA and the carboxylic group of TIB. Meanwhile, a PLA-PEG-PLA triblock copolymer and its TIB-capped derivative were also synthesized. All the samples obtained were further characterized by ^{1}H NMR and GPC measurements, as presented in Figs. S1 and S2 (See ESI). The extent of acylation calculated by comparison of the integral of the aromatic peaks of TIB groups to the methoxy or methylene peak of PEG segment exceeded 90% for all the TIB-capped derivatives, indicating the successful introduction of TIB moieties into mPEG-PLA. Table 1 lists the characteristics of mPEG-PLA diblock copolymers, PLA-PEG-PEG triblock copolymer and their TIB-capped derivatives.

Our previous studies have demonstrated that the end-group had a subtle influence on the thermogelling properties of PEG/polyester copolymers.[4b,5a] Considering this characteristic, a relatively hydrophilic PLA-PEG-PLA (P5) that was just soluble in water at a broad temperature (0-50 °C) was firstly synthesized by us. However, its TIB-capped derivative (P5-DiTIB) only precipitated in water due to the very strong hydrophobicity of TIB moieties. Fortunately, mPEG-PLA diblock copolymers suffered from a relatively weak effect of end-group compared with PLA-PEG-PLA triblock copolymers, as illustrated in Table 1. As a result, although water-soluble P2 itself just formed a free-flowing sol at the physiologically important temperature range of 10-50 °C (Fig. 2a and Fig. S3), its TIB-capped derivative (P2-TIB) exhibited a reversible sol-gel transition in water upon increase of temperature, as shown in Fig. 2a. This feature is attributed to the change of the total hydrophilicity-hydrophobicity balance of P2-TIB via the introduction of hydrophobic TIB groups. Meanwhile, different from colorless P2 aqueous solution, P2-TIB aqueous system exhibited a pale yellow color. The sol-gel transition temperature of 35% and 40% P2-TIB/water systems, which was determined via the vial inverting method,[3b, 4c] were 34 °C and 32 °C, respectively. Additionally, it can be deduced from Table 1 that TIB-capped mPEG-PLA with a fixed PEG length (550 Da) might exhibit a sol-gel transition if the PLA block length was in the range between 1220 Da and 1780 Da.

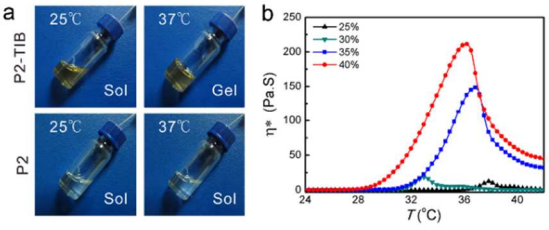

Fig. 2 (a) Upper images show the sol state at 25°C and gel state at 37°C of 40% P2-TIB aqueous solution. Bottom images exhibit just the sol sate of 40% P2 aqueous solution at the same two temperatures. (b) Viscosity η* versus temperature for P2-TIB aqueous solutions with the indicated concentrations.

To further confirm the *in situ* gel formation with increase of temperature, dynamic rheology analysis was performed to evaluate the change in viscosity of P2-TIB aqueous solutions as a function of temperature at different concentrations (Fig. 2b). At low temperatures, the viscosities of the polymer/water systems were quite low, indicating that they were in a sol state and can be easily

injected using a conventional syringe. An abrupt increase in viscosity upon heating were observed for P2-TIB solutions with higher concentrations (35 % and 40 %), demonstrating the formation of semisolid thermogel. The viscosity of 25% and 30% P2-TIB solutions did not change significantly over the range of temperature tested. This feature well coincided with the results determined via the vial inverting approach, indicating that a thermogel was able to be obtained only with polymer concentration above critical gel concentration (CGC). Meanwhile, the viscosity of both 35% and 40% P2-TIB thermogels reached 130 Pa•s at body temperature.

The strength of X-ray attenuation within objects generally reflects their radiopacity.[11] In this study, we first examined the *in vitro* radiopacity of P2-TIB aqueous solutions at various concentrations. The photographs of the samples and their corresponding Micro-CT images are shown in Fig. 3a. Al_2O_3 powder and P2 aqueous solution were chosen as the control group and the blank group, respectively. The color represents the grayscale, which reflects the radiopacity of the samples. Since the high grayscale value means the strong radiopacity, it is obvious that the radiopacity of P2-TIB aqueous solution is much higher than those of the control group and the blank group. Such a significant increasing in radiopacity is attributed to the introduction of TIB groups into mPEG-PLA diblock copolymer. Fig. 3b displays the quantitative grayscale data of different samples. P2 aqueous solution (40%) showed the smallest grayscale value of 26.8, indicating the very low radiopacity. In contrast, under the same concentration, the grayscale value of 40% P2-TIB aqueous solution increased to about 156, almost six-fold to that of 40% P2 solution and three-fold to that of Al_2O_3 powder, respectively. This feature indicates that the P2-TIB not only exhibits a temperature-responsive sol-gel transition in water, but also holds the strong radiopacity. Considering that attenuation coefficient is a characteristic value that reflects the intrinsic properties of materials such as electron density and relative atomic mass, the average attenuation coefficients of P2-TIB solutions in Micro-CT measurements were linearly fitted versus their corresponding concentrations (Fig. 3c). A good correlation coefficient R^2 (>0.99) and a positive slope (6.43×10^{-4}) were achieved, indicating the positive correlation between the radiopacity of TIB-capped mPEG-PLA and its concentration. Such a linear relation is vital for the quantitative assessment during its *in vivo* application.

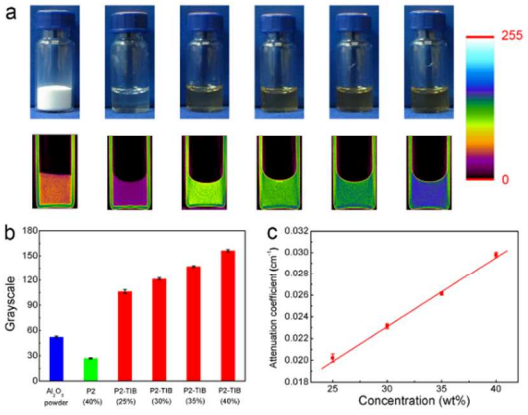

Fig. 3 (a) The optical photographs (upper) and corresponding Micro-CT images on the x-axis (bottom) of the indicated samples (from left to right: Al_2O_3 powder, 40% P2 aqueous solution, 25%, 30%, 35% and 40% P2-TIB aqueous solutions). The color represents the radiopacity of the samples. (b) The radiopacity of the indicated samples using grayscale unit. (c) The linear fitting between the average attenuation coefficients of P2-TIB aqueous solutions and their concentrations. The results were expressed as mean ± SD (n = 4).

Generally speaking, the visualized detection of implanted biomaterials *in vivo* using Micro-CT is dependent on the radiopaque difference between the implants and the surrounding tissues. In other words, the radiopaque contrast between the implants and the surrounding tissues must be high enough to clearly distinguish each other. In the current study, ICR mouse was selected as the model animal to assess the *in vivo* radiopacity of the P2-TIB thermogel. Since P2 diblock copolymer was too hydrophilic to form a thermogel in water at any temperature and concentration and thus not available as the negative control, we selected 40% P4 thermogel as the control, whose sol-gel transition temperature was close to that of 40% P2-TIB thermogel as shown in Table 1. Fig. 4a shows the Micro-CT images on z-axis after subcutaneous injection of the different samples into ICR mice. All of the polymer solutions rapidly transformed into the *in situ* thermogels under the skins, as demonstrated in Fig. S4. It was easy to distinguish 35% and 40% P2-TIB thermogels from the surrounding soft tissues with a clear boundary due to their strong radiopacity. In contrast, the radiopacity of 40% P4 thermogel was very close to that of the surrounding soft tissues, making the thermogel hard to be distinguished from the soft tissues.

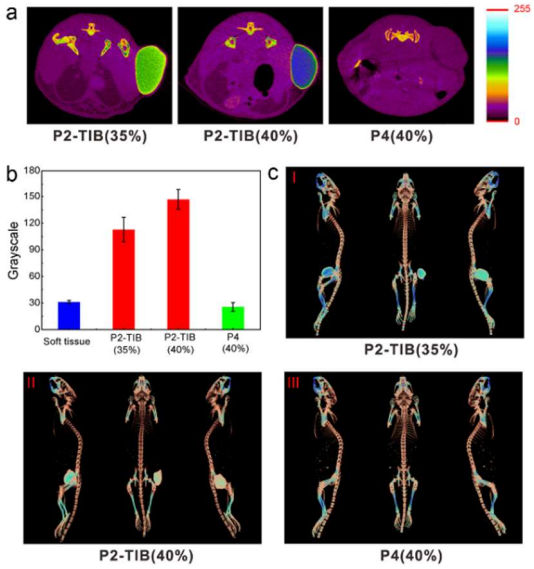

Fig. 4 (a) Sectional views of the Micro-CT imaging 0.5 h after subcutaneous injection of the indicated samples in ICR mice. (b) The *in vivo* radiopacity of the indicated samples using grayscale unit. (c) Reconstructed 3D Micro-CT images of the indicated samples in ICR mice. The radiopaque P2-TIB thermogels were clearly observed after subcutaneous injection, with skeleton as reference.

Quantitative analysis of the radiopacity was also performed for all the thermogel systems. As shown in Fig. 4b, the radiopaque P2-TIB thermogels showed the significantly high grayscale compared with the soft tissue. Meanwhile, the *in vivo* grayscale value of P2-TIB thermogel also depended on its concentration, which is well consistent with the *in vitro* results. Furthermore, the visualized morphology of P2-TIB thermogel *in vivo* was conveniently achieved by 3D reconstruction of Micro-CT images with the results shown in Fig. 4c and Video 1 in ESI. Both 35% and 40% P2-TIB thermogels with ellipsoidal shape were clearly observed in the 3D reconstruction images. In contrast, non-radiopaque P4 thermogel was not visualized in the reconstructed 3D Micro-CT images.

Next, the intraperitoneal injection of P2-TIB and P4 thermogels to ICR mice was carried out. Their corresponding Micro-CT images and reconstructed 3D images are displayed in Fig. 5a, revealing that 40% P2-TIB thermogel can be clearly distinguished from the

surrounding organs in the abdomen while 40% P4 thermogel was barely detected. Reconstructed 3D Micro-CT images further confirmed that the 40% P2-TIB thermogel in the abdomen appeared an irregular shape, implying that the P2-TIB thermogel just located at the void space between the abdominal organs. Quantitative data of grayscale also demonstrated that the 40% P2-TIB thermogel exhibited much stronger radiopacity than the surrounding abdominal organs but no significant difference was found between the 40% P4 thermogel and the surrounding organs (Fig. 5b). These *in vivo* imaging results convincingly demonstrate that TIB-capped mPEG-PLA thermogel possesses good injectability and high *in vivo* radiopacity at different administration sites.

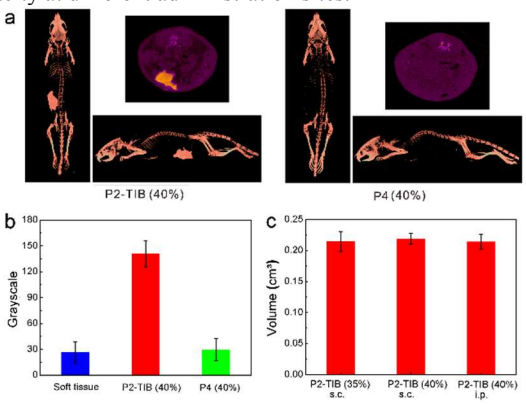

Fig. 5 (a) Sectional views and reconstructed 3D images of the *in vivo* Micro-CT imaging 0.5 h after intraperitoneal injection of the indicated samples in ICR mice. (b) The radiopacity of the indicated samples using grayscale unit. (c) Volume of the P2-TIB thermogel at different administration sites in ICR mice calculated from the reconstructed 3D images. The results were expressed as mean ± SD (n = 3). Here, s.c. means subcutaneous injection and i.p. represents intraperitoneal injection.

The *in vivo* volume of thermogel after injection was calculated using the reconstructed 3D Micro-CT images. As shown in Fig. 5c, regardless of the injection site, all of the *in vivo* volume of P2-TIB thermogel were approximately 0.22 mL. In fact, the actual volume of injection was 0.24 mL each time. Considering the residual in the syringe, the volume obtained from the micro-CT image was very close to the actual volume of injection. Such an *in situ* volumetric detection would allow non-invasive tracing of *in vivo* degradation of the implants. Additionally, no sign of acute toxicity was observed for the animals after the injection of P2-TIB thermogels at different administration sites.

In conclusion, a novel radiopaque thermogel was designed and synthesized by us for the first time. Although the mPEG-PLA diblock copolymer itself was just soluble in water, the covalent linking of hydrophobic TIB moieties to the PLA end of mPEG-PLA diblock copolymers significantly adjusted the total hydrophilicity-hydrophobicity balance of the TIB-capped mPEG-PLA, resulting in the sol-gel transition with increase of temperature. Meanwhile, the TIB-capped mPEG-PLA thermogel exhibited excellent radiopacity in both *in vitro* and *in vivo* testing. The *in vivo* 3D morphology of the thermogel at different administration sites can be conveniently constructed and the corresponding volume of injection can be accurately calculated using the Micro-CT imaging. Such an *in vivo* visualized detection provides a non-invasive method to orientate the administration site and trace the change in morphology of the implanted thermogel. These results also suggest that the injectable and radiopaque thermogel shows great potential as sustained drug delivery system at particular site, such as joint, embolization agent for endoleak treatment, tumor chemo-embolization, tissue marker, and so on.

This work was supported by the NSF of China (Grants No. 51273217 and No. 21474019), the Chinese Ministry of Science and Technology (973 Program No. 2011CB606203) and the Science and Technology Developing Foundation of Shanghai (Grants No. 12JC1402600 and No. 14441901500).

Notes and references

1 (a) H. J. Moon, D. Y. Ko, M. H. Park, M. K. Joo and B. Jeong, *Chem. Soc. Rev.*, 2012, **41**, 4860-4883; (b) Z. Y. Zhong, P. J. Dijkstra, F. J. Jan, Y. M. Kwon, Y. H. Bae and S. W. Kim, *Macromol. Chem. Phys.*, 2002, **203**, 1797-1803; (c) L. Yu and J. D. Ding, *Chem. Soc. Rev.*, 2008, **37**, 1473-1481; (d) T. Vermonden, R. Censi and W. E. Hennink, *Chem. Rev.*, 2012, **112**, 2853-2888; (e) L. Yu, W. Xu, W. J. Shen, L. P. Cao, Y. Liu, Z. S. Li and J. D. Ding, *Acta Biomater.*, 2014, **10**, 1251-1258; (f) P. Ni, Q. X. Ding, M. Fan, J. F. Liao, Z. Y. Qian, J. C. Luo, X. Q. Li, F. Luo, Z. M. Yang and Y. Q. Wei, *Biomaterials*, 2014, **35**, 236-248; (g) L. Yu, H. T. Hu, L. Chen, X. G. Bao, Y. Z. Li, L. Chen, G. H. Xu, X. J. Ye and J. D. Ding, *Biomater. Sci.*, 2014, **2**, 1100-1109; (h) T. Y. Ci, L. Chen, L. Yu and J. D. Ding, *Sci Rep*, 2014, **4**, 5473.

2 (a) M. H. Park, B. G. Choi and B. Jeong, *Adv. Funct. Mater.*, 2012, **22**, 5118-5125; (b) M. H. Park, Y. Yu, H. J. Moon, D. Y. Ko, H. S. Kim, H. Lee, K. H. Ryu and B. Jeong, *Adv. Healthc. Mater.*, 2014, **3**, 1782-1791.

3 (a) X. J. Loh, S. H. Goh and J. Li, *Biomacromolecules*, 2007, **8**, 585-593;(b) L. Yu, Z. Zhang, H. Zhang and J. D. Ding, *Biomacromolecules*, 2009, **10**, 1547-1553; (c) C. D. Liu, Z. Zhang, K. L. Liu, X. Ni and J. Li, *Soft Matter*, 2013, **9**, 787-794.

4 (a) B. Jeong, Y. H. Bae and S. W. Kim, *Macromolecules*, 1999, **32**, 7064-7069; (b) L. Yu, G. T. Chang, H. Zhang and J. D. Ding, *J. Polym. Sci., Part A: Polym. Chem.*, 2007, **45**, 1122-1133; (c) C. Chen, L. Chen, L. P. Cao, W. J. Shen, L. Yu and J. D. Ding, *RSC Adv.*, 2014, **4**, 8789-8798; (d) L. Yu, Z. Zhang and J. D. Ding, *Biomacromolecules*, 2011, **12**, 1290-1297; (e) L. Chen, T. Y. Ci, T. Li, L. Yu and J. D. Ding, *Macromolecules*, 2014, **47**, 5895-5903.

5 (a) L. Yu, H. Zhang and J. D. Ding, *Angew. Chem.-Int. Edit.*, 2006, **45**, 2232-2235; (b) A. Petit, B. Muller, P. Bruin, R. Meyboom, M. Piest, L. M. J. Kroon-Batenburg, L. G. J. de Leede, W. E. Hennink and T. Vermonden, *Acta Biomater.*, 2012, **8**, 4260-4267.

6 (a) X. Hao, M. Zhou, X. Zhang, J. Yu, J. Jie, C. Yu and X. Zhang, *Chem. Commun.*, 2014, **50**, 737-739; (b) Y. Wang and X.-P. Yan, *Chem. Commun.*, 2013, **49**, 3324-3326.

7 A. A. Appel, M. A. Anastasio, J. C. Larson and E. M. Brey, *Biomaterials*, 2013, **34**, 6615-6630.

8 A. Fouras, M. J. Kitchen, S. Dubsky, R. A. Lewis, S. B. Hooper and K. Hourigan, *J. Appl. Phys.*, 2009, **105**.

9 J.-M. Coutu, A. Fatimi, S. Berrahmoune, G. Soulez and S. Lerouge, *J. Biomed. Mater. Res. Part B*, 2013, **101B**, 153-161.

10 M. J. Sandker, A. Petit, E. M. Redout, M. Siebelt, B. Muller, P. Bruin, R. Meyboom, T. Vermonden, W. E. Hennink and H. Weinans, *Biomaterials*, 2013, **34**, 8002-8011.

11 M. H. McKetty, *Radiographics*, 1998, **18**, 151-163.